```
293      300          310         320
 |        |            |           |
CTRPNNNTRKSIHIGPGRAFYTTGEIIGDIRQAHC
         RGVPM       L A  DV  N
            NL       W    Q
            S        C    A
            T             H
            Y             P
```

図１　ヒトレトロウイルスエンベロープタンパク質のV3部分にpolymorphicなアミノ酸置換を導入し，V3に関するウイルスライブラリーを作製した．この領域は，標的細胞への侵入時にコレセプターと相互作用する．

(X4ウイルス)と相互作用することが知られており，ウイルス侵入の鍵となる分子である．従って，レトロウイルスの不活化の標的としても重要な候補となる分子のひとつである．gp120には，感染時コレセプターと直接相互作用するV3ドメインがあり，極めて多様性に富んでいることで知られている．本研究の目標は，ウイルスの不活化技術開発のために，多様な変異の組み合わせをもつウイルスを作製する．そして，そのウイルスを用いてウイルス不活化・不活化能の評価法の開発をめざす．

B. 研究方法

gp120 V3 領域（35アミノ酸残基）に臨床分離株から得られた18種類のアミノ酸変異をランダムに導入した V3 変異ライブラリーを作製した（図１）．その組み合わせは ＞２×10^4となる．このウイルスライブラリーから，45個のクローンを分離して，V3への複数の変異導入により，感染性を失っているかどうかを検討した．

C. 研究結果

ウイルスクローンのうち36%は変異導入によって感染性を失っていた．野生株と比較すると38%がその90%感染性が低下しており，18%が50%以上その感染性を失っていることがわかった．導入した変異はどれも臨床分離株から選択したものだが，組み合わせによっては，gp120の機能を失わせるのに十分であることがわかった．

このウイルスライブラリーの有用性を調べるために，R5 HIVの侵入阻害剤であるmaravirocを用いてこの薬剤に感受性の低いウイルスの選択をおこなった．実際

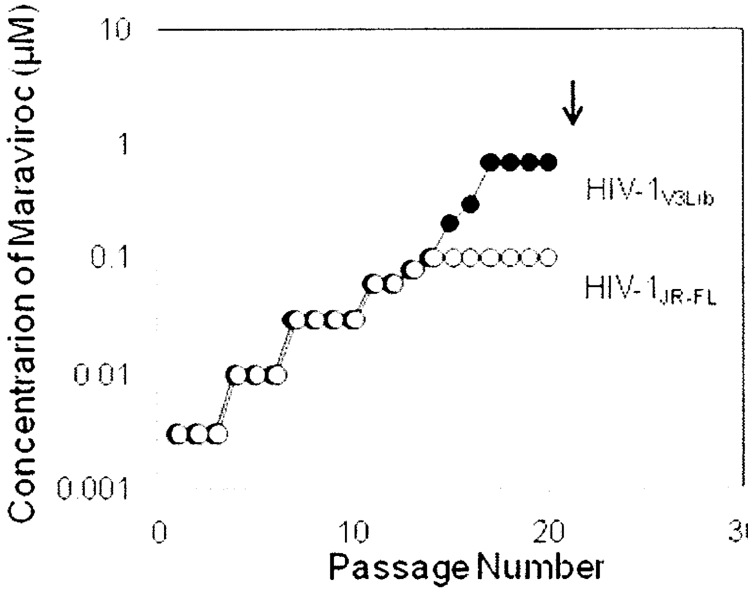

図２　ここでは選択圧として薬剤を使い、特異的なV3構造をもつウイルスが選ばれてくるかどうかを調べた. 野生株に比べて, ライブラリーウイルスからは、薬剤に強い抵抗性をもつウイルスが, 選択されてくることがわかる.

にはmaravirocによってウイルス複製が50%抑制がかかる薬剤濃度である0.3 nMから継代とともに薬剤濃度を上げていき, 17回継代したところでウイルスの培養を中止した（図２）. 最終的にmaravirocの濃度は700 nMとなり, 2300倍もの感受性の低いウイルスクローンが選択されたことになる（表１）. また選択されたウイルスのV3は5つの変異（I304V/F312W/T314A/E317D/I318V）を含んでおり多様な変異の組み合わせをもつウイルス集団は, 薬剤による選択によって単一のクローンに絞られたことになる. またV3領域以外にT199K, T275Mも見つかった.

D. 考察

導入した変異は, 効率よく各クローンに見いだされ, そのサイズも>10^7と変異の組み合わせを十分カバーする大きさであった. このことから実験系においては十分多様性に富んだウイルスポピュレーションを扱うことができるものと考えられた.

表1　選択されたウイルスの薬剤感受性を調べると抵抗性を示した.

	EC$_{50}$[a] (μM)	
	maraviroc[b]	TAK-779[b]
HIV-1$_{JR-FL}$	0.0069 ± 0.0019[c] (1.0)	0.043 ± 0.009 (1)
HIV-1$_{JR-FL-p17}$	0.055 ± 0.0055 (8)	0.15 ± 0.033 (3.5)
HIV-1$_{V3LIb}$	0.0055 ± 0.0007 (0.8)	0.025 ± 0.007 (0.6)
HIV-1$_{V3LIb-p17}$	> 10 (> 1449)	> 10 (> 233)

[a]PM1/CCR5 cells were infected at 100 TCID$_{50}$ in the presence of the CCR5 inhibitor on day 0. Cytopathic effect was determined on day 6 by the MTT method.
[b]Drug concentrations of 50% growth inhibition of the cells (CC$_{50}$) was > 10 μM.
[c]mean ± SD (n = 3).

またV3に変異をいれることで，薬剤という淘汰圧に対し，耐性をもつウイルスを比較的容易に選択することができることが示された．従ってここで用いた薬剤をウイルス不活化のための物理化学的淘汰圧と置き換えることにより，不活化に抵抗性のウイルスを分離し，その抵抗性を解析することでウイルス不活化のための条件を解明することができることが期待される．それによって不活化技術の開発につなげていけるものと考えられた．

E. 結論

今回得られたウイルスクローンからなるウイルス集団は，gp120のV3領域のみに多様な変異をもつ他は均一のウイルスライブラリーである．V3に多様な変異の組み合わせをもつウイルス集団であり，ウイルス不活化に対し，異なる反応性を持つことが予想される．今後は，温度，界面活性剤，pHなどのウイルス不活化過程に多様な変異gp120がどのような影響をもつのかを明らかにする予定である．

G. 研究発表

1. 論文発表

(1) Maeda, Y., Yusa, K., Nakano, Y., Harada, S. Involvement of inhibitory factors in the inefficient entry of HIV-1 into the human CD4 positive HUT78 cell line. *Virus Res.* 155: 368-371, 2011.

(2) Yuan, Y., Maeda, Y., Terasawa, H., Monde, K., Harada, S., Yusa, K. A Combination of Polymorphic Mutations in V3 Loop of HIV-1 gp120 Can Confer Noncompetitive Resistance to Maraviroc. *Virology, in press.*

2. 学会発表

(1) Yuan, Y., Maeda, Y., Hiromi, T., Monde, K., Yusa, K., Harada, S. Complete resistance to maraviroc in R5 HIV-1 with gp120 V3 loop mutations is affected by T199K and/or T275M in Env. 11th KUMAMOTO AIDS Seminar - GCOE Joint International Symposium, Aso, 10.6.2010. (2) 前田洋助, 中野雄介, 遊佐敬介, 原田信志. HIV-1 侵入過程のビリオン動態の可視化. 第58回に本ウイルス学会学術集会 徳島; 11.9.2010.

(3) 遊佐敬介, Yuan Yuzhe, 前田洋助, 寺沢広美, 門出和精, 原田信志. HIV-1 の gp120 V3 ループ変異による侵入阻害剤 Maraviroc高度耐性の獲得. 第58回に本ウイルス学会学術集会 徳島; 11.9.2010.

(4) 中野雄介, 前田洋助, 遊佐敬介, 原田信志. コレセプター阻害剤によるコレセプター間oligomerization修飾. 第24回日本エイズ学会学術総会 東京 11.24.2010; 2010.

(5) 遊佐敬介, Yuan Yuzhe, 前田洋助, 寺沢広美, 門出和精, 原田信志. HIV-1 の gp120 V3 ループ変異による侵入阻害剤 Maraviroc高度耐性の獲得. 第24回日本エイズ学会学術集会 東京 11.25. 2010.

H. 知的財産権の出願・登録状況

なし

研究成果の刊行に関する一覧表

雑誌

発表者氏名	論文タイトル名	発表誌名	巻号	ページ	出版年
Maeda, Y., Yusa, K., Nakano, Y., Harada, S.	Involvement of inhibitory factors in the inefficient entry of HIV-1 into the human CD4 positive HUT78 cell line.	Virus Res.	155	368-371	2011
Yuan, Y., Maeda, Y., Terasawa, H., Monde, K., Harada, S., Yusa, K.	A combination of polymorphic mutations in V3 Loop of HIV-1 gp120 Can confer noncompetitive resistance to maraviroc	Virology	*in press*		
A. Ishii-Watabe, Y. Saito, T. Suzuki, M. Tada, M. Ukaji, K. Maekawa, K. Kurose, N. Kaniwa, J. Sawada, N. Kawasaki, T. Yamaguchi, T. E. Nakajima, K. Kato, Y. Yamada, Y. Shimada, T. Yoshida, T. Ura, M. Saito, K. Muro, T. Doi, N. Fuse, T. Yoshino, A. Ohtsu, N. Saijo, T. Hamaguchi, H. Okuda, Y. Matsumura	Genetic polymorphisms of FCGRT encoding FcRn in a Japanese population and their functional analysis.	Drug Metab. Pharmacokine	25(6)	578-587	2010
Urayama, T., Sapsutthipas, S., Tsujikawa, M., Yamashita, A., Nishigaki, H., Ibrahim, MS., Hagiwara, K., Yunoki, M., Yasunaga, T., Yamaguchi, T. and Ikuta, K.	Full-Length Sequences of One Genotype 4 and Three Genotype 3 Hepatitis E Viruses in Fecal Samples from Domestic Swine in Japan.	The Open Veterinary Science Journal	4	11-19.	2010

Virus Research 155 (2011) 368–371

Contents lists available at ScienceDirect

Virus Research

journal homepage: www.elsevier.com/locate/virusres

Short communication

Involvement of inhibitory factors in the inefficient entry of HIV-1 into the human CD4 positive HUT78 cell line

Yosuke Maeda*, Keisuke Yusa, Yusuke Nakano, Shinji Harada

Department of Medical Virology, Faculty of Life Sciences, Kumamoto University, 1-1-1 Honjo, Kumamoto 860-8556, Japan

ARTICLE INFO

Article history:
Received 23 July 2010
Received in revised form 6 October 2010
Accepted 8 October 2010
Available online 20 October 2010

Key words:
HIV
Entry
T cell line
Inhibitory factors

ABSTRACT

Little is known about whether human CD4 positive T cells, the principal natural target of HIV-1, have intrinsic factors, other than the receptor/coreceptor molecules, which modulate the entry efficiency of HIV-1. In the present study, we found that human T cell lines, HUT78 and PM1, were less permissive to VSV-G-mediated HIV-1 infection compared with the Jurkat cell line. Furthermore, HUT78 cells were also less sensitive to HIV-1 Env-mediated infection, while PM1 cells became susceptible to HIV-1. Real-time PCR analyses showed that less susceptibility of the cells to HIV-1 was due to block at, or prior to, reverse transcription of viral RNA. To clarify the entry efficiency of HIV-1 into these cell lines, we analyzed the internalization of p24 Ag into the cytosolic and vesicular fractions of post-nuclear extracts at 4 h post-infection. When the cells were infected with HIV-1 pseudotyped with VSV-G, the amount of p24 Ag in the cytosolic fractions in both HUT78 and PM1 cells was lower than that observed in Jurkat cells. In the case of HIV-1 Env-mediated infection, however, PM1 cells exhibited comparable amounts of p24 Ag in the cytosolic fraction compared with Jurkat cells, while the amount of p24 Ag in HUT78 cells remained low. Heterokaryon experiments between susceptible and less susceptible cell lines suggested that some inhibitory factors counteracted VSV-G-mediated viral entry in PM1 and HUT78 cells, and HIV-1 Env-mediated viral entry in HUT78 cells.

The entry of HIV-1 into CD4 positive cells is dependent on the expression of its principle receptor CD4 and coreceptors CCR5 or CXCR4. However, it is well known that the susceptibility of CD4 positive cells to HIV-1 is dependent on the cell type even though they express comparable levels of receptors and coreceptors. The restricted replication of HIV-1 in CD4 positive cells can be partly explained by the existence of intracellular restriction factors, such as APOBEC3 and TRIM5α, both of which inhibit the post-entry steps of HIV-1 (reviewed in Zheng and Peterlin, 2005). However, it is remains to be determined whether natural targets of HIV-1, CD4 positive T cells, have intrinsic factors which modulate HIV-1 infection other than these molecules. A recent report showed that some human CD4 positive T cell lines exhibit a HIV-1 restriction phenotype at a late phase of infection (Han et al., 2008). Importantly, it has been shown that resistance to HIV-1 infection in CD4 positive T cells from exposed uninfected individuals (EU) is mediated by entry and post-entry blocks (Saez-Cirion et al., 2006). Thus, it is essential to determine whether human CD4 positive T cells have intrinsic factors which actively inhibit the entry phase of HIV-1 infection, and factors other than APOBEC3/TRIM5α that restrict the post-entry phase.

To address the differential susceptibility of HIV-1 at the early phase of infection in CD4 positive T cells, we selected the human CD4 positive T cell lines, Jurkat, HUT78 and PM1, as a model of natural target cells, CD4 positive primary T cells. To analyze the early phase of HIV-1 infection alone, a HIV-1 vector encoding GFP, in which the *env* gene is defective, was generated. Briefly, the luciferase coding region of HIV-1 pNL43LucΔenv vector (Masuda et al., 1995) was replaced with an *XhoI*/*NotI* fragment containing the *EGFP* gene from pEGFP-N1 (Takara Bio/Clontech, Tokyo, Japan) to generate pNL43GFPΔenv. To produce a GFP-reporter HIV-1 pseudotyped with VSV-G or HIV-1 NL43 (X4 HIV-1) Env, 293T cells were cotransfected with pNL43GFPΔenv and either pHEF-VSVG (Chang et al., 1999) or pCXN-NLenv (Maeda et al., 2000), as previously described (Maeda et al., 2000). The same number of cells were infected with increasing amounts of the GFP-reporter HIV-1s. The susceptibility of cells to HIV-1 was then determined two days post-infection by the percentage of GFP positive cells using flow cytometry, on a FACScan flow cytometer (BD Biosciences, Palo Alto, USA). As shown in Fig. 1A, Jurkat cells were highly permissive to HIV-1 while the HUT78 and PM1 cell lines were 10-fold and 40-fold less susceptible to HIV-1 pseudotyped with VSV-G, respectively. In contrast, when HIV-1 was pseudotyped with NL43 Env, PM1 cells became sensitive to HIV-1, while HUT78 cells remained

* Corresponding author. Tel.: +81 96 373 5131; fax: +81 96 373 5132.
E-mail addresses: ymaeda@kumamoto-u.ac.jp (Y. Maeda), yusak@nihs.go.jp (K. Yusa), 094r5222@st.kumamoto-u.ac.jp (Y. Nakano), biodef@gpo.kumamoto-u.ac.jp (S. Harada).

0168-1702/$ – see front matter © 2010 Elsevier B.V. All rights reserved.
doi:10.1016/j.virusres.2010.10.010

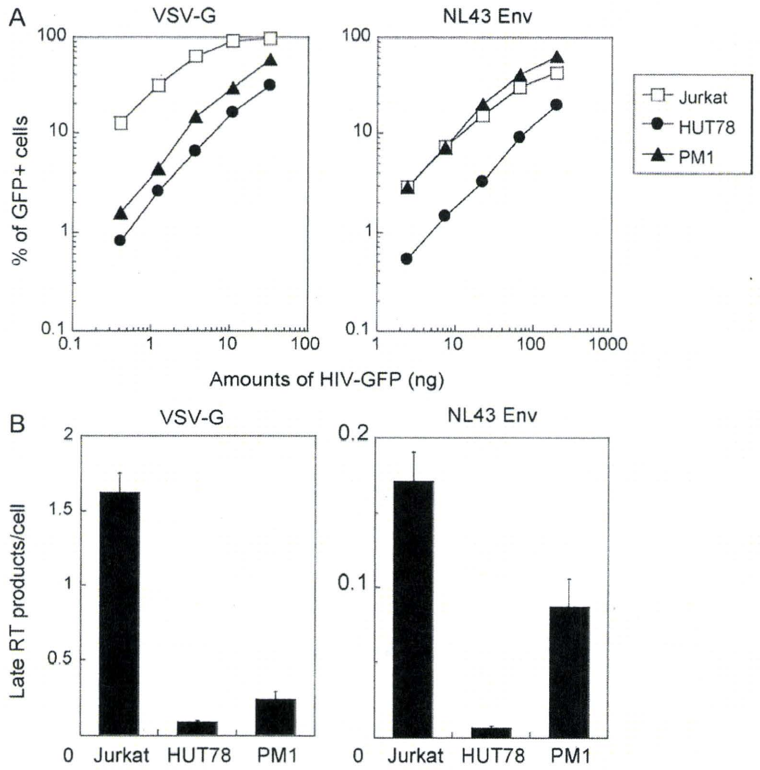

Fig. 1. Differential susceptibility of human CD4 positive T cell lines to HIV-1 infection mediated by VSV-G or HIV-1 Env. (A) The indicated cells (2×10^5 cells) were infected with increasing amounts of GFP-reporter HIV-1 pseudotyped with VSV-G or HIV-1 Env. The susceptibly of cells to HIV-1 was then analyzed two days post-infection by the percentage of GFP positive cells using flow cytometry. (B) The indicated cells (1×10^6) were infected with DNase-treated GFP-reporter HIV-1 pseudotyped with VSV-G or HIV-1 Env. After a 4-h culture at 37 °C, cells were collected and genomic DNA was extracted. DNA was analyzed for cellular apolipoprotein B or viral late RT products by real-time PCR. Dilution of plasmids containing apolipoprotein B or proviral HIV-1 clones were used to generate standard curves for quantifying PCR products. The Y-axis represents the copy number of late RT products per cell.

less permissive. Real-time PCR was then performed to quantify the number of late transcripts of these cell lines at 4 h post-infection, as previously described (Monde et al., 2007). We found that PM1 and HUT78 cells contained 6-fold and 16-fold fewer HIV-1 late reverse transcripts than Jurkat cells, respectively (Fig. 1B). When HIV-1 entry was mediated by HIV-1 Env, HUT78 cells contained 26-fold and 14-fold fewer late reverse transcripts than Jurkat and PM1 cells, respectively. These results indicated that less susceptibility of the cells to HIV-1 was due to block at, or prior to, reverse transcription of viral RNA (Fig. 1B).

To clarify whether the differential susceptibility was due to the entry efficiency of HIV-1 into the cells, we isolated the cytosolic and vesicular fractions of these cell lines 4 h post-infection, as previously described (Marechal et al., 1998). Briefly, 300 ng and 1000 ng of HIV-1 pseudotyped with VSV-G and NL43-Env were used for virus inoculation, respectively, and were incubated at 4 °C for 30 min, followed by culturing for 4 h at 37 °C. The cells were then lysed with hypotonic buffer and a Dounce homogenizer (Wheaton, Millville, NJ, USA), and the post-nuclear extracts were isolated by centrifugation at low speed to remove the nuclei. The cytosolic and vesicular fractions were then obtained by ultracentrifugation using a TL100 ultracentrifuge (Beckman Coulter, Brea, CA, USA). The amounts of p24 Ag in both fractions were determined using a p24 Ag enzyme immunoassay (EIA) (Zeptometrix, Buffalo, NY, USA) according to the manufacturer's protocol. The cytosolic and vesicular fractions of the cells infected with same amounts of p24 Ag used in EIA experiment were also applied to western blotting, as previously described (Chatterji et al., 2006), and the p24 Ag products in both fractions of these cell lines were detected using a monoclonal antibody against HIV-1 p24 Ag, VAK4 (Koito et al., 1988). In agreement with the flow cytometric and real-time PCR data, less susceptible cells had lower amounts of p24 Ag in the cytosolic fractions than susceptible cells in the case of both VSV-G and HIV-1 Env using a p24 Ag EIA (Fig. 2A) and western blotting (Fig. 2B). Since the amount of p24 Ag in the cytosolic fractions correlates with successful infection (Marechal et al., 1998), these findings strongly suggested that less susceptibility of the cell to HIV-1 via VSV-G and HIV-1 Env was largely due to inefficient entry of HIV-1 into these less sensitive cells. Notably, we found that the amount of p24 Ag in the cytosolic fractions of Jurkat cells was higher than that of the vesicular fractions, while the amount of p24 Ag in the vesicular fractions in HUT78 and PM1 cells was higher than the cytosolic fractions (Fig. 2A). Since VSV-G uses clathrin-mediated endocytosis for viral entry (Cureton et al., 2009; Johannsdottir et al., 2009; Sun et al., 2005), it seems likely that VSV-G-mediated endocytic entry of HIV-1 into HUT78 and PM1 cells partially directed towards the degradation pathway in lysosomes. Thus, it should be noted that the efficiency of VSV-G-mediated entry was dependent on the cell type, although VSV-G has been widely used as an envelope glycoprotein with broad tropism for gene therapy. On the other hand, HIV-1 Env-mediated entry was efficient in PM1 cells but remained relatively inefficient in HUT78 cells. Since these cell lines endogenously express comparable levels of CD4 and CXCR4 (see supplementary data 1), factor(s) other than the receptor and coreceptor molecules were likely to be involved in inefficient entry mediated by HIV-1 Env in HUT78 cells. HIV is known to enter CD4 positive cells via fusion between the viral and host cell membranes. Early studies have showed that viral fusion is not triggered by acidification of the endosome (McClure et al., 1988; Stein et al., 1987), indicating that viral entry mediated by HIV-1 Env does not use the endocytic route. Instead, HIV-1 Env was assumed to mediate the direct fusion of the viral and host cell plasma membranes. Thus, the direct fusion

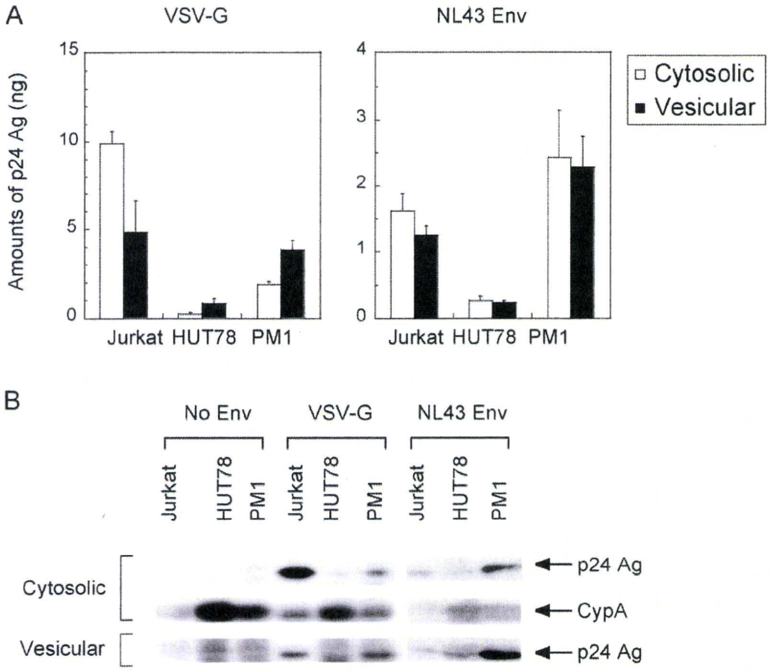

Fig. 2. Inefficient entry of HIV-1 mediated by VSV-G and HIV-1 Env. The indicated cells (1×10^7 cells) were exposed to 300 ng or 1000 ng of GFP-reporter HIV-1 pseudotyped with VSV-G or NL43 Env, respectively, for 30 min at 4 °C, followed by a 4-h at 37 °C. The infected cells were fractionated into vesicular and cytosolic extracts. The cytosolic and vesicular fractions were examined using a p24 Ag EIA (A) and western blot analysis (B). The EIA results were expressed as the total amount of p24 Ag in the cytosolic (open bar) and vesicular (closed bar) fractions from independent triplicate experiments. Western blot analysis of the cytosolic and vesicular fractions in infected cells was carried out using an anti-p24 Ag monoclonal antibody, VAK4. The cyclophilin A levels in the cytosolic fractions were used as an internal control.

route was likely to be active in PM1 cells, although the endocytic route was blocked.

To distinguish whether the inefficient entry of HIV-1 could be due to the absence of a required factor(s) or the presence of an inhibitory factor(s) in these less susceptible cell lines, we generated heterokaryons formed by fusion between sensitive and less sensitive cell lines. Jurkat, HUT78 and PM1 cells were first labeled with the fluorescent membrane dye Vybrant DiI or DiD (Invitrogen, Carlsbad, CA, USA). These differentially marked cells were then fused by polyethylene glycol (PEG) as previously described (Agarwal et al., 2006; Lech and Somia, 2007). Fused cells were then infected with GFP-reporter HIV-1 pseudotyped with VSV-G or NL43 Env. The percentage of GFP positive cells two days post-infection in both the DiI and DiD positive population indicating homo- and heterokaryons, was determined by flow cytometry. We found that homo- and heterokaryons were easily detected as the DiI and DiD double positive cell population at levels corresponding to 10–15% of the total cell population by flow cytometry after PEG-mediated fusion (Fig. 3A). The susceptibility of homokaryons to HIV-1 was similar to that of each single cell line as shown in Fig. 1A, indicating that PEG-mediated fusion did not affect susceptibility (Fig. 3B). In the heterokaryons infected with HIV-1 mediated by VSV-G, the percentage of GFP positive cells in heterokaryons between Jurkat and HUT78 cells was marginally higher than that in HUT78 homokaryons, but did not reach the level observed in Jurkat homokaryons. On the other hand, the percentage of heterokaryons between Jurkat and PM1 cells was almost the same as that in PM1 homokaryons (Fig. 3B). These results indicated that inefficient entry into PM1 and HUT78 cells mediated by VSV-G was partially explained by the presence of an inhibitory factor(s). Since the PM1

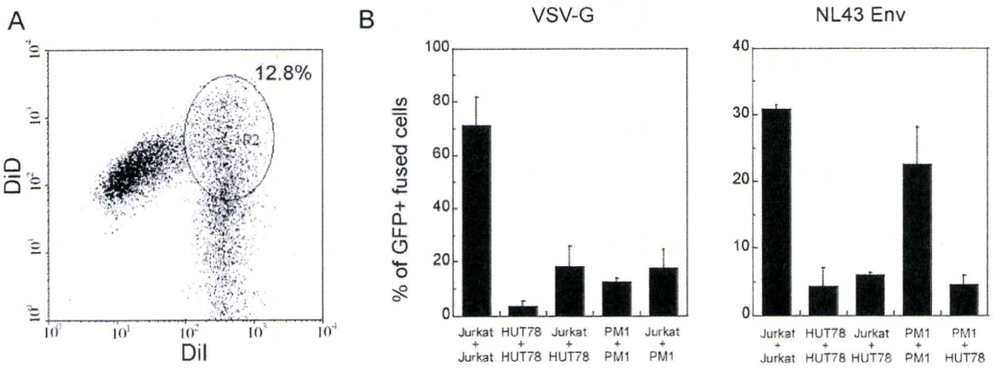

Fig. 3. Involvement of inhibitory factors in the inefficient entry of HIV-1 mediated by VSV-G and HIV-1 Env. The indicated cells were first labeled with the fluorescent membrane dye, Vybrant DiI or DiD. The differently marked cells were then fused with PEG and analyzed by flow cytometry. Homo- and heterokaryons are shown in both the DiI and DiD positive populations at levels corresponding to 10–15% of the total cell population. Representative data from flow cytometry after fusion by PEG are shown (A). The fused cells were then infected with the GFP-reporter HIV-1 pseudotyped with VSV-G and NL43 Env, and the percentage of GFP positive cells in both the DiI and DiD positive populations were determined two days post-infection by flow cytometry (B).

cell line is a derivative of the HUT78 cell line (Lusso et al., 1995), the same factor(s) is likely to block the VSV-G-mediated endocytic route in HUT78 and PM1 cells. Alternatively, it is also possible that an inhibitory factor(s) in PM1 and HUT78 cells competes for the binding of VSV-G with its receptor, although the receptor for VSV-G remains to be confirmed (Coil and Miller, 2004; Schlegel et al., 1983). Interestingly, the inefficient levels of entry mediated by HIV-1 Env in HUT78 cells were not restored by heterokaryons formed with Jurkat or PM1 cells (Fig. 3B), indicating that an inhibitory factor(s) may also play a role in HUT78 cells (Fig. 3B). Since HUT78 cells counteracted viral entry mediated by both VSV-G and HIV-1 Env, it is likely that other molecule(s) in HUT78 cells interrupted the direct fusion route mediated by HIV-1 Env. However, recent studies have suggested that HIV-1 Env also uses the endocytic pathway for viral entry into CD4 positive cells (Daecke et al., 2005; Fackler and Peterlin, 2000; Miyauchi et al., 2009) although these findings are currently under debate. Given that entry of HIV-1 into HUT78 cells was exclusively mediated by the same endocytic pathway despite the use of different Env proteins, it seems possible that the same molecule(s) may counteract viral entry mediated by both VSV-G and HIV-1 Env. However, it remains to be determined whether HIV-1 primarily uses the endocytic route for viral entry into CD4 positive T cells *in vitro* and *in vivo*.

Importantly, the findings of our study indicate that an inhibitory factor(s) counteract endocytic entry by VSV-G- and HIV-1 Env-mediated infection in HUT78 cells. The identification of this factor(s) will shed light on additional molecular mechanisms of viral entry/fusion and provide a new insight into potential therapeutic approaches for HIV-1.

Acknowledgments

We thank Irvin S.Y. Chen and Atsushi Koito for generously providing pNL43LucΔenv and VAK4, respectively. The reagent pHEF-VSVG was obtained from Lung-Ji Chang through the AIDS Research and Reference Reagent program, Division of AIDS, National Institute of Allergy and Infectious Diseases, US National Institutes of Health. Thanks are also due to Kazuaki Monde and Yuzhe Yuan for helpful discussions and Hiromi Terasawa for technical assistance. This work was supported by grants from the Ministry of Education, Culture, Sports, Science and Technology, and the Ministry of Health, Labour and Welfare, Japan.

Appendix A. Supplementary data

Supplementary data associated with this article can be found, in the online version, at doi:10.1016/j.virusres.2010.10.010.

References

Agarwal, S., Harada, J., Schreifels, J., Lech, P., Nikolai, B., Yamaguchi, T., Chanda, S.K., Somia, N.V., 2006. Isolation, characterization, and genetic complementation of a cellular mutant resistant to retroviral infection. Proc. Natl. Acad. Sci. U.S.A. 103 (43), 15933–15938.

Chang, L.J., Urlacher, V., Iwakuma, T., Cui, Y., Zucali, J., 1999. Efficacy and safety analyses of a recombinant human immunodeficiency virus type 1 derived vector system. Gene Ther. 6 (5), 715–728.

Chatterji, U., Bobardt, M.D., Gaskill, P., Sheeter, D., Fox, H., Gallay, P.A., 2006. Trim5α accelerates degradation of cytosolic capsid associated with productive HIV-1 entry. J. Biol. Chem. 281 (48), 37025–37033.

Coil, D.A., Miller, A.D., 2004. Phosphatidylserine is not the cell surface receptor for vesicular stomatitis virus. J. Virol. 78 (20), 10920–10926.

Cureton, D.K., Massol, R.H., Saffarian, S., Kirchhausen, T.L., Whelan, S.P.J., 2009. Vesicular stomatitis virus enters cells through vesicles incompletely coated with clathrin that depend upon actin for internalization. PLoS Pathog. 5 (4), e1000394.

Daecke, J., Fackler, O.T., Dittmar, M.T., Krausslich, H.G., 2005. Involvement of clathrin-mediated endocytosis in human immunodeficiency virus type 1 entry. J. Virol. 79 (3), 1581–1594.

Fackler, O.T., Peterlin, B.M., 2000. Endocytic entry of HIV-1. Curr. Biol. 10 (16), 1005–1008.

Han, Y., Wang, X., Dang, Y., Zheng, Y.H., 2008. Demonstration of a novel HIV-1 restriction phenotype from a human T cell line. PLoS One 3 (7), e2796.

Johannsdottir, H.K., Mancini, R., Kartenbeck, J., Amato, L., Helenius, A., 2009. Host cell factors and functions involved in vesicular stomatitis virus entry. J. Virol. 83 (1), 440–453.

Koito, A., Hattori, T., Matsushita, S., Maeda, Y., Nozaki, C., Sagawa, K., Takatsuki, K., 1988. Conserved immunogenic region of a major core protein (p24) of human and simian immunodeficiency viruses. AIDS Res. Hum. Retroviruses 4 (6), 409–417.

Lech, P., Somia, N.V., 2007. Isolation and characterization of human cells resistant to retrovirus infection. Retrovirology 4, 45.

Lusso, P., Cocchi, F., Balotta, C., Markham, P.D., Louie, A., Farci, P., Pal, R., Gallo, R.C., Reitz Jr., M.S., 1995. Growth of macrophage-tropic and primary human immunodeficiency virus type 1 (HIV-1) isolates in a unique CD4⁺ T-cell clone (PM1): failure to downregulate CD4 and to interfere with cell-line-tropic HIV-1. J. Virol. 69 (6), 3712–3720.

Maeda, Y., Foda, M., Matsushita, S., Harada, S., 2000. Involvement of both the V2 and V3 regions of the CCR5-tropic human immunodeficiency virus type 1 envelope in reduced sensitivity to macrophage inflammatory protein 1α. J. Virol. 74 (4), 1787–1793.

Marechal, V., Clavel, F., Heard, J.M., Schwartz, O., 1998. Cytosolic Gag p24 as an index of productive entry of human immunodeficiency virus type 1. J. Virol. 72 (3), 2208–2212.

Masuda, T., Planelles, V., Krogstad, P., Chen, I., 1995. Genetic analysis of human immunodeficiency virus type 1 integrase and the U3 att site: unusual phenotype of mutants in the zinc finger-like domain. J. Virol. 69 (11), 6687–6696.

McClure, M.O., Marsh, M., Weiss, R.A., 1988. Human immunodeficiency virus infection of CD4-bearing cells occurs by a pH-independent mechanism. EMBO J. 7 (2), 513–518.

Miyauchi, K., Kim, Y., Latinovic, O., Morozov, V., Melikyan, G.B., 2009. HIV enters cells via endocytosis and dynamin-dependent fusion with endosomes. Cell 137 (3), 433–444.

Monde, K., Maeda, Y., Tanaka, Y., Harada, S., Yusa, K., 2007. Gp120 V3-dependent impairment of R5 HIV-1 infectivity due to virion-incorporated CCR5. J. Biol. Chem. 282 (51), 36923–36932.

Saez-Cirion, A., Versmisse, P., Truong, L.X., Chakrabarti, L.A., Carpentier, W., Barre-Sinoussi, F., Scott-Algara, D., Pancino, G., 2006. Persistent resistance to HIV-1 infection in CD4 T cells from exposed uninfected Vietnamese individuals is mediated by entry and post-entry blocks. Retrovirology 3, 81.

Schlegel, R., Tralka, T.S., Willingham, M.C., Pastan, I., 1983. Inhibition of VSV binding and infectivity by phosphatidylserine: is phosphatidylserine a VSV-binding site? Cell 32 (2), 639–646.

Stein, B.S., Gowda, S.D., Lifson, J.D., Penhallow, R.C., Bensch, K.G., Engleman, E.G., 1987. pH-independent HIV entry into CD4-positive T cells via virus envelope fusion to the plasma membrane. Cell 49 (5), 659–668.

Sun, X., Yau, V.K., Briggs, B.J., Whittaker, G.R., 2005. Role of clathrin-mediated endocytosis during vesicular stomatitis virus entry into host cells. Virology 338 (1), 53–60.

Zheng, Y.H., Peterlin, B.M., 2005. Intracellular immunity to HIV-1: newly defined retroviral battles inside infected cells. Retrovirology 2, 25.

Drug Metab. Pharmacokinet. 25 (6): 578–587 (2010).

Regular Article

Genetic Polymorphisms of *FCGRT* Encoding FcRn in a Japanese Population and Their Functional Analysis

Akiko ISHII-WATABE[1,a], Yoshiro SAITO[2,3,b,*], Takuo SUZUKI[1], Minoru TADA[1], Maho UKAJI[2], Keiko MAEKAWA[2,3], Kouichi KUROSE[2,3], Nahoko KANIWA[2,3], Jun-ichi SAWADA[2,4,**], Nana KAWASAKI[1], Teruhide YAMAGUCHI[1], Takako EGUCHI NAKAJIMA[5,†], Ken KATO[5], Yasuhide YAMADA[5], Yasuhiro SHIMADA[5], Teruhiko YOSHIDA[6], Takashi URA[7], Miyuki SAITO[7], Kei MURO[7], Toshihiko DOI[8], Nozomu FUSE[8], Takayuki YOSHINO[8], Atsushi OHTSU[8,9], Nagahiro SAIJO[10,††], Tetsuya HAMAGUCHI[5], Haruhiro OKUDA[2,4] and Yasuhiro MATSUMURA[11]

[1]*Division of Biological Chemistry and Biologicals, National Institute of Health Sciences, Tokyo, Japan*
[2]*Project Team for Pharmacogenetics, National Institute of Health Sciences, Tokyo, Japan*
[3]*Division of Medicinal Safety Sciences, National Institute of Health Sciences, Tokyo, Japan*
[4]*Division of Organic Chemistry, National Institute of Health Sciences, Tokyo, Japan*
[5]*Gastrointestinal Oncology Division, National Cancer Center Hospital, Tokyo, Japan*
[6]*Genetics Division, National Cancer Center Research Institute, National Cancer Center, Tokyo, Japan*
[7]*Department of Medical Oncology, Aichi Cancer Center Hospital, Nagoya, Japan*
[8]*Division of Gastrointestinal Oncology/Digestive Endoscopy, National Cancer Center Hospital East, Kashiwa, Japan*
[9]*Director of Research Center for Innovative Oncology, National Cancer Center Hospital East, Kashiwa, Japan*
[10]*Deputy Director, National Cancer Center Hospital East, Kashiwa, Japan*
[11]*Investigative Treatment Division, National Cancer Center Hospital East, Kashiwa, Japan*
[a,b]*Akiko Ishii-Watabe and Yoshiro Saito contributed equally to this work*

Full text of this paper is available at http://www.jstage.jst.go.jp/browse/dmpk

Summary: Neonatal Fc receptor (FcRn) plays an important role in regulating IgG homeostasis in the body. Changes in FcRn expression levels or activity caused by genetic polymorphisms of *FCGRT*, which encodes FcRn, may lead to interindividual differences in pharmacokinetics of therapeutic antibodies. In this study, we sequenced the 5′-flanking region, all exons and their flanking regions of *FCGRT* from 126 Japanese subjects. Thirty-three genetic variations, including 17 novel ones, were found. Of these, two novel non-synonymous variations, 629G>A (R210Q) and 889T>A (S297T), were found as heterozygous variations. We next assessed the functional significance of the two novel non-synonymous variations by expressing wild-type and variant proteins in HeLa cells. Both variant proteins showed similar intracellular localization as well as antibody recycling efficiencies. These results suggested that at least no common functional polymorphic site with amino acid change was present in the *FCGRT* of our Japanese population.

Keywords: ***FCGRT*; neonatal Fc receptor (FcRn); genetic polymorphism; novel non-synonymous variation**

Received; July 19, 2010, Accepted; September 14, 2010, J-STAGE Advance Published Date; October 1, 2010

*To whom correspondence should be addressed: Yoshiro SAITO, PhD, *Division of Medicinal Safety Sciences, National Institute of Health Sciences, 1-18-1 Kamiyoga, Setagaya-ku, Tokyo 158-8501, Japan. Tel. +81-3-3700-9528, Fax. +81-3-3700-9788, E-mail: yoshiro@nihs.go.jp*
***Present address: Pharmaceuticals and Medical Devices Agency, Shin-Kasumigaseki Building, 3-3-2 Kasumigaseki, Chiyoda-ku, Tokyo 100-0013, Japan.*
†*Present address: Department of Clinical Oncology, St. Marianna University School of Medicine, 2-16-1 Sugao, Miyamae-ku, Kawasaki-city 216-8511, Japan.*
††*Present address: Kinki University School of Medicine, 377-2 Ohno-Higashi, Osaka-Sayama City, Osaka 589-8511, Japan.*
This study was supported in part by the Program for the Promotion of Fundamental Studies in Health Sciences from the National Institute of Biomedical Innovation, and by the Health and Labor Sciences Research Grants from the Ministry of Health, Labor and Welfare of Japan, and by KAKENHI (20590167) from the Japan Society for the Promotion of Science (JSPS).

Introduction

Neonatal Fc receptor (FcRn) is an immunoglobulin G (IgG) receptor related to major histocompatibility (MHC) class I molecules.[1,2] Like MHC class I, FcRn consists of a heavy chain with extracellular $\alpha1$, $\alpha2$, and $\alpha3$ domains followed by a transmembrane segment and a short cytoplasmic tail and non-covalently bound $\beta2$-microglobulin ($\beta2$m). FcRn binds the Fc region of monomeric IgG. The FcRn heavy chain is encoded by *FCGRT*, which is located in chromosome 19q13.3 and comprises 6 exons.

In humans, FcRn expression has been observed in a wide variety of tissues including placenta, liver, kidney and vascular endothelium.[1] FcRn has multiple roles in the body such as absorption or secretion of IgG across the intestinal mucosa, and IgG recycling from endothelial cells. With regard to antibody recycling, FcRn binds to the Fc domain of IgG at acidic pH in endosomes after endocytosis, and recycles it back to the extracellular space via the exocytic pathway, thereby protecting IgG from intracellular degradation in lysosomes.[2] This mechanism contributes to the long serum half-life of IgG, and thus, IgG recycling activity is an important function of FcRn and could contribute to the efficacy of antibody therapeutics. Indeed, we previously reported that affinities of antibody therapeutics to FcRn were closely correlated with the serum half-lives reported in clinical studies.[3] The relatively short serum half-life of Fc-fusion proteins such as etanercept, a fusion protein consisting of the extracellular ligand-binding portion of the human tumor necrosis factor receptor linked to the Fc portion of human IgG1, is thought to arise from low affinity to FcRn.[3]

Genetic polymorphisms of genes related to drug metabolism and transport are one of the crucial factors for low-molecular-weight drugs. Pharmacokinetics or pharmacodynamics of biologicals including antibody therapeutics may also be influenced by genetic polymorphisms of transport or target proteins. In this context, changes in FcRn expression levels or activity caused by genetic polymorphisms of *FCGRT* may lead to interindividual differences in pharmacokinetics of antibody therapeutics. However, reports on *FCGRT* genetic polymorphisms in Japanese populations are lacking.

Here we sequenced the 5′-flanking region, all exons and their flanking regions of *FCGRT* from 126 Japanese subjects. We then examined the functional properties of two detected non-synonymous variations using mammalian expression systems focusing on intracellular localization and antibody recycling activities.

Materials and Methods

Human genomic DNA samples: One hundred twenty-six Japanese cancer patients participated in this study. The ethical review boards of the National Cancer Center, Aichi Cancer Center and the National Institute of Health Sciences approved this study. Written informed consent was obtained from all subjects. Genomic DNA for DNA sequencing was extracted from blood leukocytes.

PCR conditions for DNA sequencing: The following sequences obtained from GenBank were used for primer design and reference sequences: NW_927240.1 (genome) and NM_004107.3 (mRNA). For sequencing, two sets of long-range PCR were performed to amplify all 6 exons from 50 ng of genomic DNA with two sets of primers (0.5 μM) designed in the promoter or intronic regions as listed in "1st PCR" of **Table 1**. We used LA-Taq with GC buffer I (0.05 U/μl, Takara Bio Inc., Shiga, Japan) to amplify from the 5′-flanking region to exon 3 and Z-Taq (0.025 U/μl, Takara Bio. Inc.) from exons 4 to 6, as described in **Table 1**. The 1st PCR conditions were 94°C for 5 min, followed by 30 cycles of 94°C for 30 sec, 60°C for 1 min, and 72°C for 2 min, and then a final extension at 72°C for 7 min for LA-Taq, and 30 cycles of 98°C for 5 sec, 55°C for 5 sec, and 72°C for 190 sec for Z-Taq. Next, each region was separately amplified in the 2nd PCR using the 1st PCR product as the template. We used LA-Taq with GC buffer I or II (0.05 U/μl) for amplifying regions from the 5′-flanking region to exon 3 and Ex-Taq (0.02 U/μl, Takara Bio. Inc.) from exons 4 to 6 as described in **Table 1**. The 2nd PCR conditions were 94°C for 5 min, followed by 30 cycles of 94°C for 30 sec, 60°C for 1 min, and 72°C for 2 min, and then a final extension at 72°C for 7 min for all regions. The PCR products were then treated with a PCR Product Pre-Sequencing Kit (USB Co., Cleveland, OH, USA) and directly sequenced on both strands using an ABI BigDye Terminator Cycle Sequencing Kit ver. 3.1 (Applied Biosystems, Foster City, CA, USA) and the sequencing primers listed in **Table 1** (Sequencing). Excess dye was removed by a DyeEx96 kit (Qiagen, Hilden, Germany) and the eluates were applied to an ABI Prism 3730xl DNA Analyzer (Applied Biosystems). All relatively low frequent variations ($n \leq 5$) were confirmed by repeated sequencing analyses of PCR products generated from original (not amplified) genomic DNA. The nucleotide positions based on the cDNA sequence were numbered from the adenine of the translational initiation site or the nearest exons.

Hardy-Weinberg equilibrium and linkage disequilibrium (LD) analyses: Hardy-Weinberg equilibrium and LD analyses were performed by SNPAlyze software ver. 7 (Dynacom Co., Yokohama, Japan). Hardy-Weinberg equilibrium was assessed by the $\chi2$ test and pairwise LDs between variations were obtained for the frequently used coefficients $|D'|$ and rho square (r^2). $|D'|$ is used to assess the probability for past recombinations, and r^2 is used as a parameter for the linkage between a pair of variations.

Table 1. Primers used for sequencing *FCGRT*

	Enzyme*	Amplified or sequenced region	Forward primer (5′ to 3′)	Reverse primer (5′ to 3′)	Amplified length (bp)
1st PCR	LA-GI	5′-flanking to Exon 3	CTCAGGCTGGTCCTTGAACTCA	ATTAGCCAGTTATGGTGGTATG	5,244
	Z	Exons 4 to 6	CAAGTGTGGTGGTGGGCACCTA	GGGAGTTCGAGACCAGCCTGAT	3,788
2nd PCR	LA-GI	5′-flanking	CTGAACCAGCTGAACGTCCACT	CTGAGCGTGGTGGTGGGCCTGT	1,058
	LA-GII		ATAGAGGTGACAGTTGCACAGC	GGTCCAGACTGACAACAATGCC	1,477
	LA-GII	Exon 1	GAGCAGCAGCCTCCCACAGGAT	ACACAAGAGGCGACAGGTGGTT	1,017
	LA-GI	Exons 2 to 3	ATTGTTGTCAGTCTGGACCG	GCTGCAGTGGGAGGCTGATGGA	1,332
	Ex	Exons 4 to 5	CCAAGGAGGTGACATCTTGAGG	CATCTCTGGGTTTCTGTCTCCA	1,383
	Ex	Exon 6	CCGCCTTGCCGCTGCTGATCCA	GAGCTGAGATCACGCAATTGTA	1,632
Sequencing		5′-flanking	CTGAACCAGCTGAACGTCCACT	CAGGGTCTGGCTCTGTCACTCA	
			GTGCAGAATAGGCAAATCTATC	AACCACATCCTTCTGCTAGGAC	
			CGGGTTCAAGCAATTCTCCTGT	TTGAGGGTGTCTGCCGCTCAGG	
			GAGCAGCAGCCTCCCACAGGAT	CCTCCTCTCTCAGACCCAGGAA	
			CCTGGGTCTGAGGGAGGAGT	CCTCCTCGTACCTGAAGAACTT	
		Exon 1	GGACTCTCAGCCTATCAAGT	ACACAAGAGGCGACAGGTGGTT	
			CCGCGGTGTCCCGGGAGGAA		
		Exons 2 to 3	GTATCTGTCCCACTGCAGTCTA	AACTGAGGCAGGTGGGCATGAC	
		Exon 4	TGAGTCTCTGTCACCTAGGAAG	AGTTAACAGCTCTTCAGACTCA	
		Exon 5	CCGCCTTGCCGCTGCTGATCCA	GTCTCTGTCCTCCCAGGTCTGT	
		Exon 6	TCAGAGAGAGGTGGAGACAGAA	GATGTATAAAACTGGCAGGTTC	
			CCTTGGATCTCCCTTCGTGGAG	TGGCTCACACTTGTAATCCCAC	
			GACGGAGTCTTGCTCTGTTGCT		

*LA-GI: LA-Taq with GC buffer I, LA-GII: LA-Taq with GC buffer II, Z: Z-Taq, Ex: Ex-Taq.

Construction of FcRn expression plasmid: Wild-type human FcRn cDNA was originally obtained from pME18SFL3 (AK075532) (Toyobo, Osaka, Japan). The coding region of FcRn cDNA subcloned into pcDNA3 was amplified by PCR, and then inserted into the EcoRI/SalI site of pEGFP-(C) plasmid. The resulting plasmid encodes hFcRn with C-terminally fused enhanced green fluorescent protein (EGFP) containing the eight amino acid-linker peptide VDSRGSRV between the two proteins. Mutations were introduced by an inverse PCR method. Primers consisted of 5′-AAG GCC CAA CCC AGC AGC CCT GGC TTT-3′ (forward) and 5′-CAG GCG CAT GGA GGG GGG CC CTT CCA-3′ (reverse) for R210Q, 5′-TCC ACC GTC CTC GTG GTG GGA ATC GTC-3′ (forward) and 5′-CTT GGC TGG AGA TTC CAG CTC CAC CCT-3′ (reverse) for S297T. The underlines indicate the mutated nucleotides. The variant plasmids were sequenced on both strands for the entire cDNA region to confirm the introduction of the mutation only at the target sites. Human β2 microglobulin (β2m) cDNA was obtained from pME18SFL3 (FCC106E07) (Toyobo). β2m cDNA was subcloned into pcDNA3.1/
Hygro. The β2m construct was used because FcRn becomes a heterodimer with β2m, which is necessary for the proper intracellular localization of FcRn.[4,5)]

Cell culture and plasmid transfection: HeLa cells were cultured in DMEM (Sigma-Aldrich, St. Louis, MO, USA) supplemented with 10% fetal calf serum (Nichirei, Tokyo, Japan). The plasmids encoding the wild-type or variant FcRn fused with EGFP along with the plasmid encoding β2m were transfected into HeLa cells using Lipofectamine 2000 reagent (Invitrogen, Carlsbad, CA, USA) according to the manufacturer's protocol. Plasmids encoding wild-type or variant FcRn fused with EGFP were used for all experiments, including the intracellular localization and antibody recycling activity of FcRn.

Western blot analysis: Wild-type and variant FcRn-EGFP transfected into HeLa cells in 35-mm-diameter dishes were lysed with 500 μL of RIPA buffer [50 mM Tris HCl (pH 7.6), 150 mM NaCl, 1% Nonidet P-40 and 0.25% sodium deoxycholate] supplemented with protease inhibitors (Nacalai Tesque, Kyoto, Japan). After incubation on ice for 30 min, the lysates were centrifuged at 15,000 rpm at 4°C for 20 min. An aliquot (3 μL) of the supernatant was diluted in SDS-sample buffer and applied to 10% SDS-polyacrylamide gel. After electrophoresis, separated proteins were transferred onto polyvinylidene fluoride membrane. Immunochemical detection of FcRn-EGFP proteins was performed using rabbit anti-human FcRn antibody raised against a peptide antigen (residues 135–148, LNGEEFMNFDLKQG). Visualization of the proteins was achieved with horseradish peroxidase-conjugated anti-rabbit IgG antibody (Cell Signaling Technology, Danvers, MA, USA) and the ECL Plus Western blotting detection reagent (GE Healthcare Bio-Sciences AB, Uppsala, Sweden). Protein band densities measured by LAS-3000 (Fuji Film, Kanagawa, Japan) were quantified with Multi Gauge software (Fuji Film).

The relative expression levels are shown as means ± SD of three separate transfection experiments. To verify that the samples were evenly loaded, the blot was reprobed with anti-glyceraldehyde-3-phosphate dehydrogenase (G3PDH) antibody (R&D Systems, Minneapolis, MN, USA).

Fluorescent labeling of antibodies: As a model antibody, we used infliximab, a clinically used chimeric anti-human TNFα antibody which has the Fc domain of human IgG1. The binding of infliximab to human FcRn was shown by surface plasmon resonance analysis in our previous study.[3] Infliximab, kindly provided by Tanabe Pharmaceutical Co. Ltd. (Osaka Japan), was labeled with CypHer5 (GE Healthcare Bio-Sciences, Uppsala, Sweden) by incubating with CypHer5E mono NHS ester in PBS containing 0.5 M Na_2CO_3 (pH 8.3) for 1 hr at room temperature. After the reaction, unbound dye was removed by dialysis in PBS. The protein concentration and degree of labeling were determined by spectrophotometry. IgY (Jackson Immuno Research Laboratories, West Grove, PA, USA) was also labeled with CypHer5 and used in control experiments.

Imaging with fluorescence microscopy: HeLa cells transfected with wild-type or variant FcRn-EGFP cDNA and the β2m cDNA were cultured on 35-mm poly-L-lysine-coated glass-bottom dishes (0.08–0.12 mm thickness) (Matsunami, Osaka, Japan) for 2–4 days. The intracellular localization analyses of wild-type and variant FcRn-EGFP were carried out by confocal laser scanning fluorescence microscopy using a Carl Zeiss LSM510 system (Carl Zeiss, Jena, Germany). For co-localization experiments, wild-type or variant FcRn-EGFP-transfected HeLa cells were incubated with CypHer5-labeled infliximab diluted in cell culture medium containing 200 mM sodium phosphate buffer (pH 6.0) for 2–3 hr at 37°C. Note that throughout this study, the cell culture media used for incubation with the labeled antibody was acidified (pH 6.0) to obtain enhanced incorporation of antibodies into the cells, as reported previously.[6,7] The fluorescent signal was observed in neutral pH medium after washing the cells twice. The 488- and 633-nm laser lines were used to image FcRn-EGFP and CypHer5 labeled-infliximab, respectively.

Biotin labeling of antibodies: Infliximab and IgY were labeled with biotin using EZ-link sulfo-NHS-biotin (Pierce, Rockford, IL, USA). Antibodies and sulfo-NHS-biotin were mixed at the molar ratio of 1:20 and incubated for 60 min at room temperature. Biotinylated antibodies were purified using Zeba desalt spin column (Pierce). Protein concentration was determined by BCA protein assay (Pierce) using bovine serum albumin as a standard.

Recycling assay: HeLa cells were transfected with the wild-type or variant FcRn-EGFP construct along with the β2m construct. The day after transfection, cells were seeded on 96-well plates at 4×10^4 cells/well. After further culturing for one day, recycling assays were performed. Hanks' balanced salt solutions (HBSS) (pH 6.0 and 7.4) were prepared supplemented with 10 mM MES (pH 6.0) and 10 mM Hepes (pH 7.4). The cells were washed with HBSS (pH 7.4) and pre-incubated with HBSS (pH 7.4) for 30 min at 37°C. After washing with HBSS, 10 μg/ml of biotinylated infliximab diluted in HBSS (pH 6.0) containing 0.5% fish gelatin was added to each well. The cells were incubated at 37°C for 1 hr to allow the antibody to be incorporated into the cells. Cells were then washed five times with HBSS (pH 7.4). Then, HBSS (pH 7.4) supplemented with 2% ultra-low IgG FCS (Invitrogen) was added to each well and incubated at 37°C for the indicated periods of time. The supernatant was collected and subjected to ELISA for quantitating the recycled antibody. In order to determine the amount of biotinylated infliximab incorporated into the cells during the 1-hr incubation at 37°C, cells were lysed using RIPA buffer supplemented with protease inhibitors (Nacalai Tesque, Kyoto, Japan) after washing five times with HBSS, and the lysate was subjected to ELISA. Biotinylated IgY was also used as a negative control in some experiments.

Enzyme linked immunosorbent assay (ELISA) for biotinylated antibody: NeutrAvidin (Pierce, Rockford, IL) was bound on Maxisorp 96-well black plates (Thermo Fisher Scientific, Roskilde, Denmark) using IMMUNO-TEK ELISA construction system (ZeptoMetrix, Buffalo, NY, USA). Supernatants or lysates obtained from the recycling assay were applied on the wells and incubated for 16 hr at 4°C. The plates were washed three times with Tris-buffered saline (pH 7.6) containing 0.1% Tween-20 (TBST). Peroxidase-conjugated goat anti-human IgG (Pierce) diluted with TBST was added to the plate and incubated for 1 hr at room temperature. After washing three times with TBST, chemiluminescent reagent (SuperSignal ELISA Femto, Pierce) was added and incubated for 1 min at room temperature. The chemiluminescent signal was detected using an ARVO 1420 multilabel counter (Perkin Elmer, Waltham MA, USA). When the amount of biotinylated IgY was measured, peroxidase-conjugated rabbit anti-chicken IgY (Promega, Madison, WI, USA) was used. For generation of a standard curve, 0.1 to 10 ng/ml of biotinylated corresponding protein was used.

Results

***FCGRT* variations found in a Japanese population:** Thirty-three genetic variations were found, including 17 novel ones, in 126 Japanese subjects (**Table 2**). Of these variations, 14 were located in the 5′-flanking region, 4 (2 synonymous and 2 non-synonymous) in the coding exons, 13 in the introns, 1 in the 3′-untranslated region (UTR), and 1 in the 3′-flanking region. All detected variations were in Hardy-Weinberg equilibrium

Table 2. Summary of *FCGRT* variations detected in this study

SNP ID		Location	Position		Nucleotide change	Amino acid change or known VNTR	Frequency	
This Study	dbSNP (NCBI) or reference		NW_927240.1	From the translational initiation site or from the end of the nearest exon				95% Confidence interval
MPJ6_FRT001[a]		5′-flanking	1557122	−2230	agaacctgaactA > Ccctgaccagcag		0.004	0.000–0.012
MPJ6_FRT002[a]			1557195	−2157	gggtgtcttgcaC > Actgtcatcccag		0.008	0.000–0.019
MPJ6_FRT003	rs78889190		1557207	−2145	cctgtcatcccaG > Ctgctttgggagg		0.020	0.003–0.037
MPJ6_FRT004[a]			1557221	−2131	gctttgggaggcC > Taaggtgggaggc		0.004	0.000–0.012
MPJ6_FRT005[a]			1557498_1557505	−1854_−1847	ggaaggaaggaaGGAAGGAA/-ggaggcaaggaa		0.024	0.005–0.043
MPJ6_FRT006	rs60964075		1557502_1557505	−1850_−1847	ggaaggaaggaaGGAA/-ggaggcaaggaa		0.103	0.066–0.141
MPJ6_FRT007	rs60964075		1557505_1557506	−1847_−1846	ggaaggaaggaaggaa-/GGAAggaggcaaggaa		0.099	0.062–0.136
MPJ6_FRT008[a]			1557505_1557506	−1847_−1846	ggaaggaaggaaggaa-/GGAAGGAAggaggcaaggaa		0.020	0.003–0.037
MPJ6_FRT009[a]			1557506	−1846	ggaaggaaggaaG > Agaggcaaggaag		0.004	0.000–0.012
MPJ6_FRT010[a]			1557540_1557547	−1812_−1805	aaggaaggaaggAAGGAAGG/-aggcaaggaagg		0.004	0.000–0.012
MPJ6_FRT011	rs2335534		1557671	−1681	tctgggagcagcG > Agctgtttaacgg		0.028	0.007–0.048
MPJ6_FRT012[a]			1558366	−986	gatacagaggggT > Gaggaggaggatc		0.004	0.000–0.012
MPJ6_FRT013	ref. 8		1558963_1558999	−389_−353	cgagggtagagcGGTTGGGGGCCCGGACTCCTGG GTCCGAGGGTAGAGC/-ggttgggggccc	VNTR3 > VNTR2	0.032	0.010–0.053
MPJ6_FRT014[a]			1559173	−179	actgagatccagT > Gtcaggggtgaaa		0.028	0.007–0.048
MPJ6_FRT015	rs59774409	Intron 1	1559442	IVS1 + 18	ggccgctccgggC > Tcagggccctgct		0.028	0.007–0.048
MPJ6_FRT016[a]			1559453	IVS1 + 29	gccagggccctgC > Ttgcaggcgggcg		0.147	0.103–0.191
MPJ6_FRT017	rs11551281	Exon 2	1559885	126[b]	ctcgcctgccccG > Tgggactcctgcc	Pro42Pro	0.044	0.018–0.069
MPJ6_FRT018	rs2878342	Exon 3	1560418	582[b]	ggagaggggccgC > Tggaaacctggag	Arg194Arg	0.028	0.007–0.048
MPJ6_FRT019[a]		Exon 4	1570485	629[b]	gcctgaaggcccG > Aacccagcagccc	Arg210Gln	0.004	0.000–0.012
MPJ6_FRT020	rs3810194	Intron 4	1570734	IVS4 + 7	agctgggtgaggT > Ccccgccaggtgg		0.048	0.021–0.074
MPJ6_FRT021	rs1132990		1570857	IVS4 + 130	gccttgaacctcA > Gcgcctgtcagtg		0.048	0.021–0.074
MPJ6_FRT022[a]			1570915	IVS4 + 188	ccaactgccttcC > Tgtctcctgctgc		0.020	0.003–0.037
MPJ6_FRT023	rs10525267		1571020_1571025	IVS4 + 293_+ 298	tgctgctgctgcTGCTGC/-gggtcttcctgg		0.083	0.049–0.117
MPJ6_FRT024[a]			1571170	IVS4–238	ctggcacagcccC > Tgccttgccgctg		0.020	0.003–0.037
MPJ6_FRT025	rs73582442		1571235	IVS4–173	gctggttcttacG > Atccaacctgggg		0.048	0.021–0.074
MPJ6_FRT026	rs73582446		1571314	IVS4–94	gctggaatctccG > Aaggctgggaggg		0.048	0.021–0.074
MPJ6_FRT027[a]		Exon 5	1571425	889[b]	ccagccaagtccT > Accgtgctcgtgg	Ser297Thr	0.020	0.003–0.037
MPJ6_FRT028	rs55662447	Intron 5	1571614_1571615	IVS5 + 90_+ 91	agagacccagagAG/-gggggacagaga		0.028	0.007–0.048
MPJ6_FRT029[a]			1571615	IVS5 + 91	gagacccagagaG > Tgggggacagaga		0.004	0.000–0.012
MPJ6_FRT030	rs77741672		1571691	IVS5 + 167	gagaggggacgG > Cagacagagaccc		0.151	0.107–0.195
MPJ6_FRT031[a]			1571915	IVS5–46	gtcagacccagaG > Acgcctcagagat		0.020	0.003–0.037
MPJ6_FRT032	rs14769	3′-UTR	1572276	1304 (*206)[c]	taacacgagtttG > Aggcccgaatcag		0.044	0.018–0.069
MPJ6_FRT033[a]		3′-flanking	1572364	1312 + 80 (*214 + 80)[d]	tgggcctcggatC > Ttctcctacaggt		0.004	0.000–0.012

[a]Novel variations detected in this study.
[b]Positions in cDNA (NM_004107.3).
[c]Numbered from the termination codon TGA.
[d]Positions were shown as 1312 (*214) (final base of exon 6) + bases from the end of exon 6.

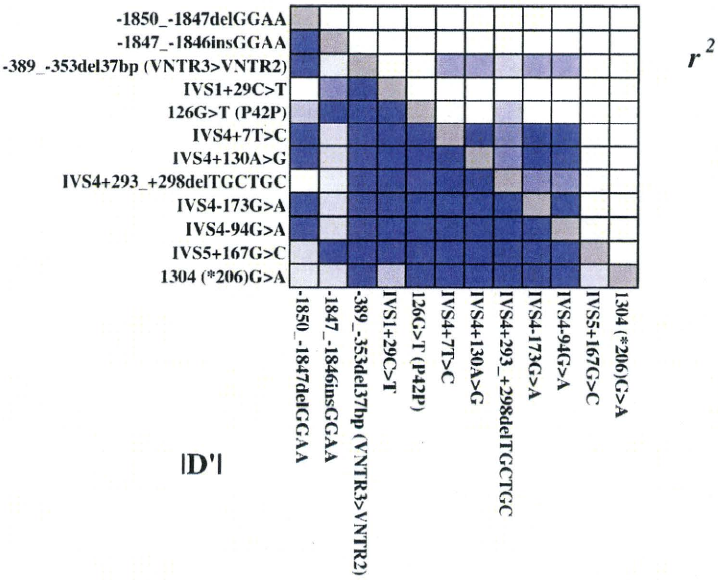

Fig. 1. Linkage disequilibrium (LD) analysis of *FCGRT*
Pairwise LD is expressed as r^2 (upper right) and |D'| (lower left) values (from 0 to 1) by 10-graded blue colors. A denser color represents closer linkage.

($p \geq 0.05$). Two novel non-synonymous variations, 629G > A (R210Q) and 889T > A (S297T), were found as heterozygotes. The allele frequencies were 0.004 for R210Q and 0.020 for S297T. The functional significance of these non-synonymous variations was explored *in vitro* in the following sections. The other coding variations were previously reported synonymous variations. A variable number of tandem repeats (VNTR) was detected in the 5′-flanking region as was found in Caucasian subjects,[8] and the frequencies of VNTR3 (with 3 repeats) and VNTR2 were 0.968 and 0.032, respectively. A short tandem repeat of GGAA was also detected in the 5′-flanking region with a repeat number of 8 (frequency: 0.024), 9 (0.103), 10 (0.754), 11 (0.099) and 12 (0.020). With the 12 detected variations with ≥0.03 frequencies, linkage disequilibrium (LD) was analyzed using |D′| and r^2 values (**Fig. 1**). Because of relatively weak linkage between the variations in r^2 values, haplotype analysis was not performed.

Intracellular localization of FcRn variants: Two novel non-synonymous variations, R210Q and S297T, were functionally tested using a mammalian expression system. First, relative expression levels of wild-type and variant FcRn proteins were evaluated by Western blotting. As shown in **Figure 2**, similar levels of the proteins were detected in the three FcRn constructs, and we did not find any statistically significant differences ($p > 0.05$) between the wild-type and the two variants assessed by Dunnett's multiple comparison test when normalized by the expression levels of glyceraldehyde-3-phosphate dehydrogenase as a control. When the wild-type levels were

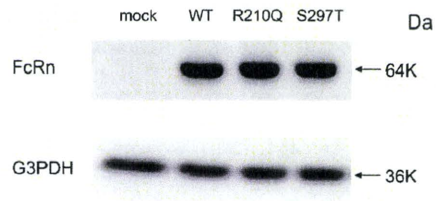

Fig. 2. Western blotting of wild-type and variant FcRns
Cell lysates obtained from the HeLa cells transfected with wild-type or either of the two variant FcRn-EGFP plasmids were subjected to electrophoresis, followed by transfer to the membrane. Detection of FcRn-EGFP was performed as described in Materials and Methods. One representative data of three independent transfections is shown. The FcRn band (64 KDa) consists of 37 KDa of FcRn and 27 KDa of EGFP. Glyceraldehyde-3-phosphate dehydrogenase (G3PDH) levels were used for normalization of the lysate proteins applied to electrophoretic gels.

set as 100%, R210Q and S297T levels were 95.08 ± 12.38% and 93.94 ± 13.24%, respectively.

In order to examine the differences of intracellular localization between wild-type FcRn and its variants, each EGFP fusion construct together with a human β2m construct was transfected into HeLa cells, and fluorescent images were observed by confocal microscopy. There have been several studies reporting the intracellular localization or trafficking of FcRn using fluorescent protein-tagged FcRn.[9-12] N- and C-terminally tagged FcRn showed similar localization.[13] Since FcRn is a type I membrane protein, N-terminal amino acid residues including R210 and S297 were located in the extracellular

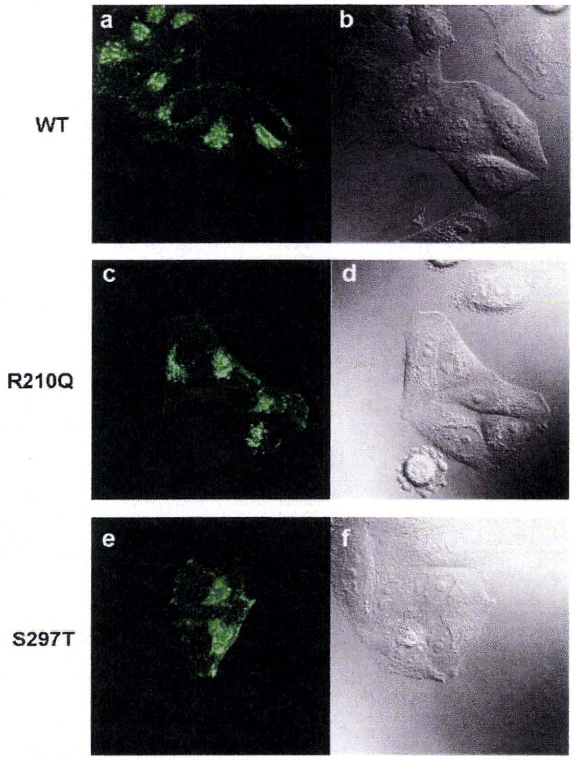

Fig. 3. Intracellular localization of wild-type (WT) and variant FcRns in HeLa cells
HeLa cells were transfected with wild-type (a) or variant (c; R210Q, e; S297T) FcRn-EGFP. The intracellular localization of FcRn-EGFP was observed by confocal laser scanning fluorescence microscopy. Differential interference contrast images of the field are also shown (b, d, f).

or intraluminal region. Therefore, we chose a C-terminal EGFP tag located in the cytoplasmic region of FcRn in order to minimize the effect of the fluorescent tag on the structural environment around the mutation sites.

As shown in **Figure 3a**, the fluorescent signal of wild-type FcRn-EGFP was located primarily in intracellular vesicular components, especially in the perinuclear region. Similar localization was observed for R210Q and S297T variants (**Figs. 3c** and **3e**), suggesting that these amino acid mutations do not affect the intracellular localization of FcRn.

Intracellular co-localization of FcRn variants and incorporated antibody: We then examined the co-localization of the incorporated CypHer5-labeled infliximab and FcRn-EGFP. The binding of CypHer5-labeled infliximab to FcRn was confirmed beforehand (data not shown).

As shown in **Figure 4**, co-localization of FcRn-EGFP and CypHer5-labeled infliximab in intracellular vesicular compartments was observed in HeLa cells expressing wild-type or variant FcRn. Since the fluorescence intensity of CypHer5 increases in acidic pH,[14] the observed fluorescent signal can indicate that CypHer5-labeled infliximab is localized in intracellular acidic compartments such as endosomes. Since the fluorescent images were obtained by confocal microscopy from cells which were washed with neutral pH media, the fluorescence is thought to be derived from incorporated antibodies and not from cell surface-bound antibodies. Therefore, these results showed that both types of FcRn variant, as well as wild-type FcRn, were in acidic endosomes in which incorporated antibodies localized.

Antibody recycling activity of FcRn variants: In order to elucidate the antibody recycling activity of wild-type and variant FcRn, we established the ELISA for biotinylated antibody (infliximab in this study), and measured the amount of recycled antibody from wild-type or variant FcRn-transfected cells. The binding of biotinylated infliximab to FcRn was confirmed by surface plasmon resonance (SPR) analysis (data not shown).

As shown in **Figure 5b**, recycled biotinylated infliximab was detected when the biotinylated infliximab had been loaded to the HeLa cells transfected with wild-type FcRn. The recycling was not detected in mock-transfected cells (**Fig. 5a**), showing that recycling was dependent on expression of FcRn. When the cells were incubated at 4°C for incorporation or recycling, the antibody was not detected in the supernatant. Therefore, recycling was mediated by intracellular trafficking of antibody and not by nonspecific mechanisms. As shown in **Figures 5c** and **5d**, similar levels of antibody recycling were also observed in HeLa cells transfected with either variant FcRn, suggesting similar IgG binding and intracellular trafficking properties of variant FcRns to those of wild-type FcRn. **Figure 6** shows the time course of antibody recycling from cells transfected with wild-type or variant FcRn. The amount of incorporated antibody was measured using the cell lysate at 0 min, and it is noteworthy that no statistical differences assessed by Dunnett's multiple comparison test were observed in the amount of incorporated antibodies between wild-type and either variant FcRn at time 0 (data not shown). The amount of recycled antibody at each time point was expressed as a percentage of the initially incorporated antibody. There was no significant difference between wild-type and the variant FcRns in the amount of recycled antibody, suggesting that these amino acid substitutions do not affect the antibody recycling activity of FcRn.

Discussion

In general, antibody therapeutics have longer half-lives than those of chemical drugs, and the $T_{1/2}$ of IgGs, except for IgG3, in humans is around 21 days. IgG1, IgG2 and IgG4, which are currently used isoforms for antibody therapeutics, have high affinities for FcRn.[15] Escaping from intracellular degradation by binding to FcRn has shown to contribute to this long half-life of the IgGs.

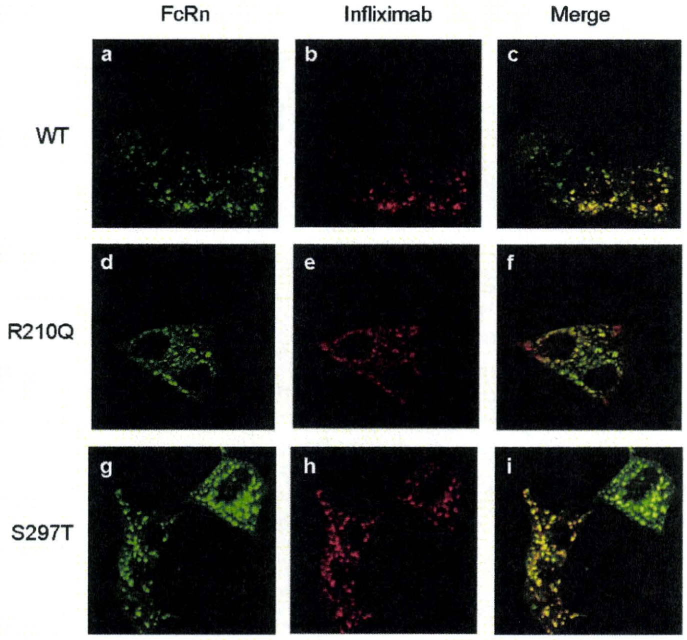

Fig. 4. Co-localization of CypHer5-labeled infliximab and FcRn in HeLa cells expressing wild-type (WT) or a variant FcRn
HeLa cells transfected with wild-type (a, b, c), or variant (d, e, f; R210Q, g, h, i; S297T) FcRn-EGFP were incubated with CypHer5-labeled infliximab in cell culture media containing sodium phosphate buffer (pH. 6.0) for 2–3 hr. After washing the cells twice with neutral pH medium, the fluorescent signal was observed. Panels (a, d, g) and (b, e, h) show the intracellular localization of FcRn-EGFP and the incorporated CypHer5-labeled infliximab, respectively. In panels (c, f, i) the fluorescent signal of FcRn-EGFP was merged with that of CypHer5-labeled infliximab.

Large interindividual variations in pharmacokinetic parameters have been reported for at least several antibody therapeutics. For example, trough concentrations in repetitive dosing of antibodies were reported to show 5.6-fold interindividual differences in 22 palivizumab-treated patients,[16] 18.2-fold differences in 16 cetuximab-treated patients,[17] and over 70-fold differences in 86 infliximab-treated patients.[18] In addition, large percent coefficients of variation were reported for $T_{1/2}$, such as 72.0% for gemtuzumab ozogamicin[19] and 76.4% for basiliximab,[20] after second dose of their treatments. We presumed that changes in FcRn expression levels and function caused by genetic variations of *FCGRT* may lead to these interindividual differences in pharmacokinetics of antibody therapeutics.

In order to identify genetic polymorphisms of *FCGRT*, we sequenced genomic DNA from 126 Japanese subjects. A total of 33 genetic variations, including 17 novel ones, were detected. A VNTR was detected in the 5′-flanking region, as was the case in Caucasian subjects reported previously.[8] Although a recent study showed that no significant impact was observed in the rates of maternal-fetal IgG transfer,[21] VNTR3 is known to be associated with 1.66-fold higher transcriptional activity than VNTR2 *in vitro*. In addition, monocytes with VNTR3/3 showed increased binding of IgG compared to those with 2/3.[8] Thus, this variation may contribute to the interindividual differences in pharmacokinetics of antibody therapeutics. The allele frequency of VNTR2 in Japanese (0.032) was lower than that in Caucasians (0.075).[8]

In this study, two novel nonsynonymous variations were found and their functional significance was assessed *in vitro* using a mammalian expression system. However, the two FcRn variants did not show any changes in intracellular localization or recycling, suggesting that the two nonsynonymous substitutions found in a Japanese population probably do not contribute to the interindividual variations in the pharmacokinetics of antibody therapeutics. Since FcRn function is important for maintenance of IgG levels as well as maternal-fetal IgG transfer, functionally-affecting genetic variations might be few to retain its functional capability.

Amino acid residues of human FcRn that interact with IgG were reported to be E138, E139, D153 and W154, in the $\alpha 2$ domain.[1] (Amino acid numbers shown in this paper include the signal peptide.). The electrostatic binding of these anionic amino acid residues in FcRn with H310 and H435 in IgG, which has an isoelectric point of pH 7.6, defines the strict pH-dependent binding of IgG to FcRn.[22] The variant amino acid residues identified in this study, R210Q and S297T, are both located in the $\alpha 3$ domain of FcRn. According to the predicted higher order structure,[1] R210 and S297 are located very close to the

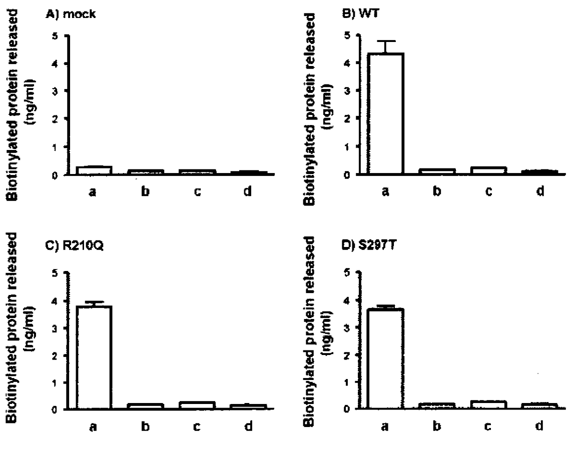

Column	a	b	c	d
Reagents	Infliximab			IgY
Loading Temp. (°C)	37	4	37	37
Recycling Temp. (°C)	37	37	4	37

Fig. 5. Recycling of biotinylated antibodies from wild-type (WT) or variant FcRn-transfected HeLa cells

HeLa cells transfected with wild-type or a variant FcRn were incubated for 1 hr with biotinylated infliximab. After washing, the cells were further incubated for 2 hr. The amount of recycled protein in the supernatant was determined by ELISA. Experimental conditions are shown in the table. For the samples shown as columns a-c, biotinylated infliximab was loaded, whereas biotinylated IgY was used for d. The temperature for antibody loading was 37°C (a, c, d) or 4°C (b). The temperature for recycling antibodies from antibody-loaded cells was 37°C (a, b, d) or 4°C (c).

transmembrane region that is distant from the IgG binding site. Considering the results obtained here, where no difference in antibody recycling activity between wild-type and each variant FcRn was detected *in vitro*, the amino acid substitutions identified in a Japanese population may not have significant impact on structural and functional properties of FcRn. Although FcRn is known to bind with albumin as well as IgG, the albumin binding site of FcRn has been identified as H189, which also is located in the $\alpha 2$ domain.[23] The polymorphic sites are also far from the albumin binding site. However, the effect of amino acid substitutions R210Q and S297T on the albumin recycling activity via FcRn should be determined in a future study.

In the present study, we used HeLa cells to examine the localization and recycling activity of FcRn variants. Since endogenous expression of FcRn protein in HeLa cells has not been detected,[24] we considered HeLa cells suitable for examining the antibody recycling activity of variant FcRn since the background responses are negligible. In fact, as shown in **Figure 5**, antibody recycling was detected only in FcRn-transfected cells. Therefore, we concluded that HeLa cells can be used as a suitable

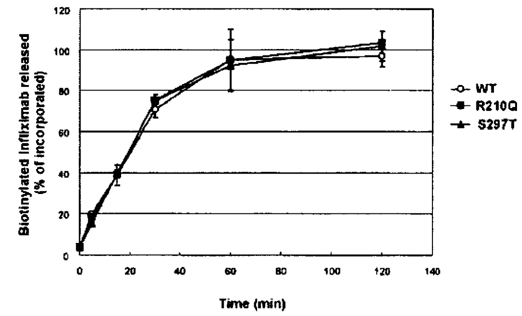

Fig. 6. Quantitative analyses of recycling of biotinylated infliximab; Time course of release of the biotinylated infliximab incorporated into the HeLa cells transfected with wild-type (WT) or variant FcRn

HeLa cells transfected with wild-type or a variant FcRn were incubated for 1 hr with biotinylated infliximab. After washing, cells were further incubated for the indicated periods of time. The amount of recycled protein was determined by ELISA. The amount of recycled antibody at each time point was expressed as a percentage of the initially incorporated antibody at time 0.

model for evaluating the function of variant FcRn proteins.

Our results suggested that at least no common functional polymorphic site with amino acid change was present in *FCGRT* in our Japanese population. Since FcRn function is important for maintenance of IgG levels, there may be few functionally-affecting genetic variations. Further analysis is necessary for the functional significance of transcriptional regulatory regions.

Acknowledgement: We thank Ms. Chie Sudo for secretarial assistance.

References

1) Andersen, J. T. and Sandlie, I.: The versatile MHC class I-related FcRn protects IgG and albumin from degradation: implications for development of new diagnostics and therapeutics. *Drug Metab. Pharmacokinet.*, **24**: 318–332 (2009).
2) Lobo, E. D., Hansen, R. J. and Balthasar, J. P.: Antibody pharmacokinetics and pharmacodynamics. *J. Pharm. Sci.*, **93**: 2645–2668 (2004).
3) Suzuki, T., Ishii-Watabe, A., Tada, M., Kobayashi, T., Kanayasu-Toyoda, T., Kawanishi, T. and Yamaguchi, T.: Importance of neonatal FcR in regulating the serum half-life of therapeutic proteins containing the Fc domain of human IgG1: a comparative study of the affinity of monoclonal antibodies and Fc-fusion proteins to human neonatal FcR. *J. Immunol.*, **184**: 1968–1976 (2010).
4) Claypool, S. M., Dickinson, B. L., Yoshida, M., Lencer, W. I. and Blumberg, R. S.: Functional reconstitution of human FcRn in Madin-Darby canine kidney cells requires co-expressed human beta 2-microglobulin. *J. Biol. Chem.*, **277**: 28038–28050 (2002).
5) Praetor, A. and Hunziker, W.: Beta(2)-microglobulin is important for cell surface expression and pH-dependent IgG bind-

ing of human FcRn. *J. Cell. Sci.*, **115**: 2389–2397 (2002).
6) Tesar, D. B., Tiangco, N. E. and Bjorkman, P. J.: Ligand valency affects transcytosis, recycling and intracellular trafficking mediated by the neonatal Fc receptor. *Traffic*, **7**: 1127–1142 (2006).
7) Kamei, D. T., Lao, B. J., Ricci, M. S., Deshpande, R., Xu, H., Tidor, B. and Lauffenburger, D. A.: Quantitative methods for developing Fc mutants with extended half-lives. *Biotechnol. Bioeng.*, **92**: 748–760 (2005).
8) Sachs, U. J., Socher, I., Braeunlich, C. G., Kroll, H., Bein, G. and Santoso, S.: A variable number of tandem repeats polymorphism influences the transcriptional activity of the neonatal Fc receptor alpha-chain promoter. *Immunology*, **119**: 83–89 (2006).
9) Goebl, N. A., Babbey, C. M., Datta-Mannan, A., Witcher, D. R., Wroblewski, V. J. and Dunn, K. W.: Neonatal Fc receptor mediates internalization of Fc in transfected human endothelial cells. *Mol. Biol. Cell.*, **19**: 5490–5505 (2008).
10) Ober, R. J., Martinez, C., Lai, X., Zhou, J. and Ward, E. S.: Exocytosis of IgG as mediated by the receptor, FcRn: an analysis at the single-molecule level. *Proc. Natl. Acad. Sci. U.S.A.*, **101**: 11076–11081 (2004).
11) Ober, R. J., Martinez, C., Vaccaro, C., Zhou, J. and Ward, E. S.: Visualizing the site and dynamics of IgG salvage by the MHC class I-related receptor, FcRn. *J. Immunol.*, **172**: 2021–2029 (2004).
12) Ward, E. S., Martinez, C., Vaccaro, C., Zhou, J., Tang, Q. and Ober, R. J.: From sorting endosomes to exocytosis: association of Rab4 and Rab11 GTPases with the Fc receptor, FcRn, during recycling. *Mol. Biol. Cell.*, **16**: 2028–2038 (2005).
13) Gan, Z., Ram, S., Vaccaro, C., Ober, R. J. and Ward, E. S.: Analyses of the recycling receptor, FcRn, in live cells reveal novel pathways for lysosomal delivery. *Traffic*, **10**: 600–614 (2009).
14) Mark, S. B., Burns, D. D., Cooper, M. E. and Gregory, S. J.: A pH sensitive fluorescent cyanine dye for biological applications. *Chem. Commun.*, **23**: 2323–2324 (2000).
15) Ternant, D. and Paintaud, G.: Pharmacokinetics and concentration-effect relationships of therapeutic monoclonal antibodies and fusion proteins. *Expert Opin. Biol. Ther.*, **5 Suppl 1**: S37–47 (2005).
16) Subramanian, K. N., Weisman, L. E., Rhodes, T., Ariagno, R., Sanchez, P. J., Steichen, J., Givner, L. B., Jennings, T. L., Top, F. H. Jr, Carlin, D. and Connor, E.: Safety, tolerance and pharmacokinetics of a humanized monoclonal antibody to respiratory syncytial virus in premature infants and infants with bronchopulmonary dysplasia. MEDI-493 Study Group. *Pediatr. Infect. Dis. J.*, **17**: 110–115 (1998).
17) Cèzè, N., Ternant, D., Piller, F., Degenne, D., Azzopardi, N., Dorval, E., Watier, H., Lecomte, T. and Paintaud, G.: An enzyme-linked immunosorbent assay for therapeutic drug monitoring of cetuximab. *Ther. Drug Monit.*, **31**: 597–601 (2009).
18) St Clair, E. W., Wagner, C. L., Fasanmade, A. A., Wang, B., Schaible, T., Kavanaugh, A. and Keystone, E. C.: The relationship of serum infliximab concentrations to clinical improvement in rheumatoid arthritis: results from ATTRACT, a multicenter, randomized, double-blind, placebo-controlled trial. *Arthritis Rheum.*, **46**: 1451–1459 (2002).
19) Dowell, J. A., Korth-Bradley, J., Liu, H., King, S. P. and Berger, M. S.: Pharmacokinetics of gemtuzumab ozogamicin, an antibody-targeted chemotherapy agent for the treatment of patients with acute myeloid leukemia in first relapse. *J. Clin. Pharmacol.*, **41**: 1206–1214 (2001).
20) Kovarik, J. M., Nashan, B., Neuhaus, P., Clavien, P. A., Gerbeau, C., Hall, M. L. and Korn, A.: A population pharmacokinetic screen to identify demographic-clinical covariates of basiliximab in liver transplantation. *Clin. Pharmacol. Ther.*, **69**: 201–209 (2001).
21) Freiberger, T., Ravcuková, B., Grodecká, L., Kurecová, B., Jarkovský, J., Bartonková, D., Thon, V. and Litzman, J.: No association of FCRN promoter VNTR polymorphism with the rate of maternal-fetal IgG transfer. *J. Reprod. Immunol.*, **85**: 193–197 (2010).
22) Vaughn, D. E., Milburn, C. M., Penny, D. M., Martin, W. L., Johnson, J. L. and Bjorkman, P. J.: Identification of critical IgG binding epitopes on the neonatal Fc receptor. *J. Mol. Biol.*, **274**: 597–607 (1997).
23) West, A. P., Jr. and Bjorkman, P. J.: Crystal structure and immunoglobulin G binding properties of the human major histocompatibility complex-related Fc receptor. *Biochemistry*, **39**: 9698–9708 (2000).
24) Liu, X., Ye, L., Christianson, G. J., Yang, J. Q., Roopenian, D. C. and Zhu, X.: NF-kappaB signaling regulates functional expression of the MHC class I-related neonatal Fc receptor for IgG via intronic binding sequences. *J. Immunol.*, **179**: 2999–3011 (2007).

Full-Length Sequences of One Genotype 4 and Three Genotype 3 Hepatitis E Viruses in Fecal Samples from Domestic Swine in Japan

Takeru Urayama[1,2], Sompong Sapsutthipas[1], Muneo Tsujikawa[2], Akifumi Yamashita[3], Hiromi Nishigaki[2], Madiha S. Ibrahim[1,4], Katsuro Hagiwara[5], Mikihiro Yunoki[1,2], Teruo Yasunaga[3], Teruhide Yamaguchi[6] and Kazuyoshi Ikuta[*,1]

[1]*Department of Virology, International Center for Infectious Disease Control, Research Institute for Microbial Diseases, Osaka University, Suita, Osaka 565-0871, Japan*

[2]*Infectious Pathogen Research Group, Osaka Laboratory, Benesis Corporation, Yodogawa-ku, Osaka 532-8505, Japan*

[3]*Department of Genome Informatics, Genome Information Research Center, Research Institute for Microbial Diseases, Osaka University, Suita, Osaka 565-0871, Japan*

[4]*Department of Microbiology, Faculty of Veterinary Medicine, Damanhour branch, EL-Bostan, Alexandria University, Alexandria, Egypt*

[5]*Department of Veterinary Microbiology, School of Veterinary Medicine, Rakuno Gakuen University, Ebetsu, Hokkaido 069-8501, Japan*

[6]*National Institute of Health Sciences, Division of Biological Chemistry and Biologicals, Setagaya-ku, Tokyo 158-8501, Japan*

Abstract: The Hepatitis E virus (HEV) induces zoonotic infections and causes hepatitis. In Japan, HEV occurs in deer, wild boar and swine, and genotype (G)3 and G4 have been isolated from domestic swine. We previously reported that HEV isolates from a total of 320 swine fecal samples from 32 farms in Japan could be predominantly classified into four clusters: three G3 ($G3_{JP}$, $G3_{SP}$ and $G3_{US}$) and one G4 ($G4_{JP}$). In this study, we performed full-length sequencing of four representative HEVs, one from each of the clusters. We found significant nucleotide variation throughout the sequences within a genotype, but not within each cluster. However, we found few variations at the amino acid level. Most of the highly conserved regions within genotypes were concentrated in the overlapping region of open reading frame (ORF)2 and ORF3, while most of the variable regions were within the ORF1 V region. This region was variable even at the amino acid level. Essentially, this region was highly conserved among G3 clusters, with some more dissimilarities between $G3_{SP}$ and the other two clusters, $G3_{JP}$ and $G3_{US}$. The regions conserved and variable across genotypes had virtually the same positions as those within genotypes, but were much narrower and wider, respectively. For the latter, ORF1 V and P regions were especially variable. Finally, we focused on the sequence conservation in the region widely used for primer and probe sets to detect HEV infections.

Keywords: HEV, full-length sequence, swine, feces, Japan.

INTRODUCTION

Several microbial agents induce hepatitis, but only HEV causes zoonotic hepatitis, mainly through food-borne transmission from domestic swine, wild boar and wild deer *via* the ingestion of uncooked or undercooked meat [1-5].

HEV is a non-enveloped small (27-34 nm in diameter) virus of the genus Hepevirus in the family *Hepeviridae* [6]. It contains single-stranded, positive-sense RNA of approximately 7.3 kilobases and its sequences have been classified into G1 to G4 [6, 7].

*Address correspondence to this author at the Department of Virology, International Center for Infectious Disease Control, Research Institute for Microbial Diseases, Osaka University, 3-1 Yamadaoka, Suita, Osaka 565-0871, Japan; Tel.: +81 6 6879 8307; Fax: +81 6 6879 8310;
E-mail: ikuta@biken.osaka-u.ac.jp

In Japan, a high prevalence of swine anti-HEV (71%) among swine aged 3-6 months and a high rate of viremia (11%) among swine of 2-4 months have been reported [8, 9], and two types of HEV are mainly circulating among pigs and humans. One type consists of three clusters of G3 ($G3_{JP}$, $G3_{SP}$ and $G3_{US}$), and the other consists of one cluster of G4 ($G4_{JP}$), which correspond to subgenotypes 3b, 3e, 3a and 4c, respectively [10]. In this study, HEVs representative of these four clusters isolated from swine feces were analyzed and their genomic and amino acid sequences compared.

MATERIALS AND METHODS

Sampling

A total of 320 fecal samples from 32 commercial pig farms (1 sample from each of the pig houses on individual farms) in Japan were processed for the partial purification of HEV as reported [11].